

Tropical principal component analysis on the space of ultrametrics

Robert Page

Department of Operations Research, Naval Postgraduate School
and

Ruriko Yoshida*

Department of Operations Research, Naval Postgraduate School
and

Leon Zhang

Department of Mathematics, University of California, Berkeley

November 26, 2019

Abstract

In 2019, Yoshida et al. introduced a notion of tropical principal component analysis (PCA). The output is a tropical polytope with a fixed number of vertices that best fits the data. We here apply tropical PCA to dimension reduction and visualization of data sampled from the space of phylogenetic trees. Our main results are twofold: the existence of a tropical cell decomposition into regions of fixed tree topology and the development of a stochastic optimization method to estimate the tropical PCA using a Markov Chain Monte Carlo (MCMC) approach. This method performs well with simulation studies, and it is applied to three empirical datasets: Apicomplexa and African coelacanth genomes as well as sequences of hemagglutinin for influenza from New York.

Keywords: Phylogenetics, Phylogenomics, Tree Spaces, Unsupervised Learning

1 Introduction

New technologies allow for the generation of genetic sequences cheaply and quickly. However, it can be challenging to analyze datasets of collections of phylogenetic trees due to their high

*The authors gratefully acknowledge the support of National Science Foundation for partially supporting R.Y. (DMS 1916037) and L.Z. (NSF Graduate Research Fellowship). The authors also thank Prof. Bernd Sturmfels for his useful comments.

dimensionality and the complex structure of the space of phylogenetic trees with a fixed number of leaves in which the data lie.

Principal component analysis (PCA) is one of the most popular methods to reduce dimensionality of input data and to visualize them. Classical PCA takes data points in a high-dimensional Euclidean space and represents them in a lower-dimensional plane in such a way that the residual sum of squares is minimized. We cannot directly apply the classical PCA to a set of phylogenetic trees because the space of phylogenetic trees with a fixed number of leaves is not Euclidean; it is a union of lower dimensional polyhedral cones in $\mathbb{R}^{\binom{m}{2}}$, where m is the number of leaves.

Nye showed an algorithm in [Nye, (2011)] to compute the first order principal component over the space of phylogenetic trees of m leaves. He defines the first order principal components as the end points of the unique shortest connecting paths, or geodesics, defined by the CAT(0)-metric introduced by Billera-Holmes-Vogtman (BHV) over the tree space of phylogenetic trees with fixed labeled leaves [Billera, et al. (2001)]. Nye in [Nye, (2011)] used a convex hull of two points, i.e., the geodesic, on the tree space as the first order PCA. However, this idea does not generalize to higher order principal components with the BHV metric as Lin et al. [Lin et al. (2017)] showed that the convex hull of three points with the BHV metric over the tree space can have arbitrarily high dimension.

On the other hand the tropical metric in tree space defined by tropical convexity in the max-plus algebra is well-studied and well-behaved [Maclagan and Sturmfels (2015)]. For example, the dimension of the convex hull of s tropical points is at most $s - 1$. In 2019, Yoshida et al. in [Yoshida et al. (2019)] defined a tropical PCA under the tropical metric with the max-plus tropical arithmetic in two ways: the best-fit Stiefel tropical linear space of fixed dimension closest to the data points in the tropical projective torus, and the best-fit tropical polytope with a fixed number of vertices closest to the data points. The authors showed that the latter object can be written as a mixed-integer programming problem to compute them, and they applied the second definition to datasets consisting of collections of phylogenetic trees. Nevertheless, exactly computing the best-fit tropical polytope can be expensive due to the high-dimensionality of the mixed-integer programming problem.

This paper focuses on the same approach to tropical PCA as a tropical polytope over the space of equidistant trees with a fixed set of leaves. In order to use tropical PCA to visualize a

dataset of phylogenetic trees, we show the existence of a decomposition of the tropical PCA into regions of unchanging tree topology deriving intrinsically from tropical geometry in Section 3. In Section 4 we propose a heuristic method to compute a tropical PCA as a tropical polytope over a space of rooted phylogenetic trees with a fixed number of leaves. To show its performance, we conduct intensive simulation studies with the proposed method in Section 5. We end this paper in Section 6 with computational experiments on three datasets consisting of Apicomplexa and African coelacanth genomes as well as sequences of hemagglutinin for influenza.

2 Tropical basics

In this section we review some basics of tropical arithmetic and tropical geometry pertaining to our setting. See [Maclagan and Sturmfels (2015)] or [Joswig (2017)] for more detail.

Definition 2.1 (Tropical arithmetic operations). *Throughout this paper we will perform arithmetic in the max-plus tropical semiring $(\mathbb{R} \cup \{-\infty\}, \oplus, \odot)$. In this tropical semiring, we define the basic tropical arithmetic operations of addition and multiplication as:*

$$a \oplus b := \max\{a, b\}, \quad a \odot b := a + b \quad \text{where } a, b \in \mathbb{R} \cup \{-\infty\}.$$

Note that $-\infty$ is the identity element under addition and 0 is the identity element under multiplication.

Definition 2.2 (Tropical scalar multiplication and vector addition). *For any scalars $a, b \in \mathbb{R} \cup \{-\infty\}$ and for any vectors $v = (v_1, \dots, v_e), w = (w_1, \dots, w_e) \in (\mathbb{R} \cup \{-\infty\})^e$, we define tropical scalar multiplication and tropical vector addition as follows:*

$$a \odot v = (a + v_1, a + v_2, \dots, a + v_e)$$

$$a \odot v \oplus b \odot w = (\max\{a + v_1, b + w_1\}, \dots, \max\{a + v_e, b + w_e\}).$$

Throughout this paper we consider the *tropical projective torus* $\mathbb{R}^e/\mathbb{R}\mathbf{1}$, where $\mathbf{1} := (1, 1, \dots, 1)$ is the all-ones vector.

Definition 2.3 (Generalized Hilbert projective metric). *For any two points $v, w \in \mathbb{R}^e/\mathbb{R}\mathbf{1}$, the tropical distance $d_{\text{tr}}(v, w)$ between $v = (v_1, \dots, v_e)$ and $w = (w_1, \dots, w_e)$ is defined as:*

$$d_{\text{tr}}(v, w) = \max_{i,j} \{ |v_i - w_i - v_j + w_j| : 1 \leq i < j \leq e \}. \quad (1)$$

This distance measure is a metric in $\mathbb{R}^e/\mathbb{R}\mathbf{1}$ and it is also known as the generalized Hilbert projective metric [Akian et al. (2011), §2.2], [Cohen et al. (2004), §3.3].

Definition 2.4. A subset $S \subset \mathbb{R}^e$ is called *tropically convex* if it contains the point $a \odot x \oplus b \odot y$ for any $x, y \in S$ and any $a, b \in \mathbb{R}$. The *tropical convex hull* or *tropical polytope* $\text{tconv}(V)$ of a finite subset $V \subset \mathbb{R}^e$ is the smallest tropically convex subset containing $V \subset \mathbb{R}^e$. The tropical convex hull of V can be written as the set of all tropical linear combinations

$$\text{tconv}(V) = \{a_1 \odot v_1 \oplus a_2 \odot v_2 \oplus \cdots \oplus a_r \odot v_r : v_1, \dots, v_r \in V \text{ and } a_1, \dots, a_r \in \mathbb{R}\}.$$

Any tropically convex subset S of \mathbb{R}^e is closed under tropical scalar multiplication, $\mathbb{R} \odot S \subseteq S$.

Finally, a subset of $\mathbb{R}^e/\mathbb{R}\mathbf{1}$ is said to be *tropically convex* if it is the quotient of a tropically convex subset of \mathbb{R}^e .

Definition 2.5. Consider a tropical polytope $\mathcal{P} = \text{tconv}(D^{(1)}, D^{(2)}, \dots, D^{(s)})$. The $D^{(i)}$ are points in $\mathbb{R}^e/\mathbb{R}\mathbf{1}$. We have

$$\pi_{\mathcal{P}}(D) = \lambda_1 \odot D^{(1)} \oplus \lambda_2 \odot D^{(2)} \oplus \cdots \oplus \lambda_s \odot D^{(s)}, \quad \text{where } \lambda_k = \min(D - D^{(k)}). \quad (2)$$

This formula appears in [Maclagan and Sturmfels (2015), (5.2.3)]. It allows us to easily project an ultrametric D (or any other point in \mathbb{R}^e) onto the tropical convex hull of s given ultrametrics.

Definition 2.6. Let $\mathcal{P} = \text{tconv}(D^{(1)}, \dots, D^{(s)}) \subseteq \mathbb{R}^e/\mathbb{R}\mathbf{1}$ be a tropical polytope. Each point x in $\mathbb{R}^e/\mathbb{R}\mathbf{1}$ has a type $S = (S_1, \dots, S_e)$ according to \mathcal{P} , where an index i is in S_j if

$$D_j^{(i)} - x_j = \max(D_1^{(i)} - x_1, \dots, D_e^{(i)} - x_e).$$

The tropical polytope \mathcal{P} consists of all points x whose type $S = (S_1, \dots, S_e)$ has all S_i nonempty. Each collection of points with the same type is called a cell.

Example 2.7. Consider the five points $D^{(1)} = (0, 0, 0)$, $D^{(2)} = (0, 3, 0)$, $D^{(3)} = (0, 3, 3)$, $D^{(4)} = (0, 1, 2)$, and $D^{(5)} = (0, 2, 1)$. The tropical convex hull of the first four points and of all five points are presented below, along with the decomposition of the polytope into cells.

2.1 Space of ultrametrics

Next we describe some basics on phylogenetic trees and review an interpretation of the space of equidistant trees as a tropical linear space.

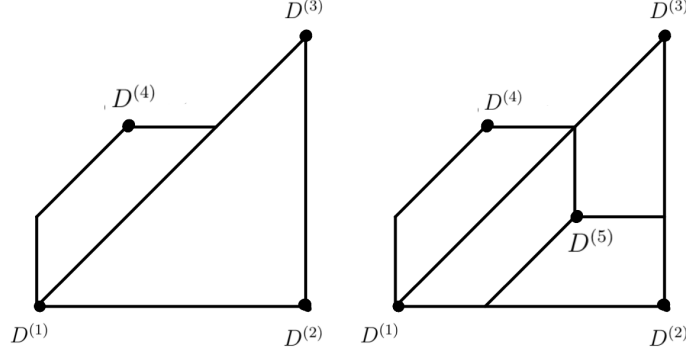


Figure 1: The two tropical polytopes of Example 2.7. Note that we visualize the tropical projective torus $\mathbb{R}^e/\mathbb{R}\mathbf{1}$ by forcing the first coordinate of each point to be 0.

Definition 2.8. Let $T = (V, E)$ be a tree with leaves with labels $[m] := \{1, \dots, m\}$ but no labels on internal nodes in T . We call such a tree a *phylogenetic tree*. An *equidistant tree* is a rooted phylogenetic tree such that a total branch length from its root to each leaf is the same.

Definition 2.9. A dissimilarity map d is a function $d : [m] \times [m] \rightarrow \mathbb{R}_{\geq 0}$ such that $d(i, i) = 0$ and $d(i, j) = d(j, i) \geq 0$ for each $i, j \in [m]$. If a dissimilarity map d satisfies a triangle inequality, i.e., $d(i, j) \leq d(i, k) + d(k, j)$ for all $i, j, k \in [m]$, then we call d a *metric*. We can represent a dissimilarity map d by an $m \times m$ matrix D whose (i, j) th entry is d_{ij} . Because D is clearly symmetric and all diagonal entries are zeros, we can regard d as a vector in $\mathbb{R}^e = \mathbb{R}^{\binom{m}{2}}$.

Note that if it is clear, for convenience, we write d_{ij} for $d(i, j)$.

Definition 2.10. Let T be a phylogenetic tree with m leaves labeled with the elements of $[m]$, and assign a length $\ell_e \in \mathbb{R}$ to each edge e of T . Define $d : [m] \times [m] \rightarrow \mathbb{R}$ such that d_{ij} is the total length of the unique path from leaf i to leaf j . We call a function d obtained in this way a *tree distance*. If, furthermore, each entry of the distance matrix D is nonnegative, then d is in fact a *metric*. We call such a tree distance a *tree metric*. As before, we can embed D into \mathbb{R}^e .

Definition 2.11. Let $d : [m] \times [m] \rightarrow \mathbb{R}_{\geq 0}$ be a metric which satisfies the following strengthening of the triangle inequality for each choice of $i, j, k \in [m]$:

$$d(i, k) \leq \max(d(i, j), d(j, k)).$$

We call such a metric an *ultrametric*. Let \mathcal{U}_m denote the collection of all ultrametries in $\mathbb{R}^e/\mathbb{R}\mathbf{1}$.

Remark 2.12. *It is well-known that a distance matrix is a tree metric for an equidistant tree if and only if it is ultrametric.*

Therefore, we view \mathcal{U}_m as the space of equidistant trees with fixed leaf labels. For the expert in tropical geometry the following theorem shows an explicit description of the space of equidistant trees with fixed labels of leaves.

Theorem 2.13 ([Develin and Sturmfels (2004)]). *Let L_m be the subspace of \mathbb{R}^e defined by the linear equations $x_{ij} - x_{ik} + x_{jk} = 0$ for $1 \leq i < j < k \leq m$. Let $\text{Trop}(L_m) \subseteq \mathbb{R}^e/\mathbb{R}\mathbf{1}$ be the tropicalization of the linear space with points $(v_{12}, v_{13}, \dots, v_{m-1,m})$ such that $\max(v_{ij}, v_{ik}, v_{jk})$ is obtained at least twice for all triples $i, j, k \in [m]$.*

Then the image of \mathcal{U}_m in the tropical projective torus $\mathbb{R}^e/\mathbb{R}\mathbf{1}$ coincides with $\text{Trop}(L_m)$.

Therefore, the space of equidistant trees with fixed labels of leaves is a tropical linear space defined by tropical equations. Figure 2 shows a space of ultrametrics for $m = 3$. This is a one-dimensional tropical linear space.

Example 2.14. *For $m = 3$, the space of ultrametrics \mathcal{U}_3 is shown in Figure 2. This is a tropical linear space defined by the tropical condition that $\max(v_{12}, v_{13}, v_{23})$ is attained twice.*

3 Properties of tropical PCA

We finally recall our notion of tropical PCA. It is important that we can interpret the tropical PCA in terms of equidistant trees. Therefore, we seek to prove properties about its interpretation.

Definition 3.1. *Let $\mathcal{P} = \text{tconv}(D^{(1)}, \dots, D^{(s)}) \subseteq \mathbb{R}^e/\mathbb{R}\mathbf{1}$ be a tropical polytope with its vertices $\{D^{(1)}, \dots, D^{(s)}\} \subset \mathbb{R}^e/\mathbb{R}\mathbf{1}$ and let $S = \{u_1, \dots, u_n\}$ be a sample from the space of ultrametrics \mathcal{U}_m . Let $\Pi_{\mathcal{P}}(S) := \sum_{i=1}^{|S|} d_{\text{tr}}(u_i, u'_i)$, where u'_i is the tropical projection of u_i onto a tropical polytope \mathcal{P} . Then the vertices $D^{(1)}, \dots, D^{(s)}$ of the tropical polytope \mathcal{P} are called the $(s - 1)$ -th order tropical principal components of S if the tropical polytope \mathcal{P} minimizes $\Pi_{\mathcal{P}}(S)$ over all possible tropical polytopes with s many vertices.*

One nice property of our tropical PCA is that each cell comprises ultrametrics of the same tree topology.

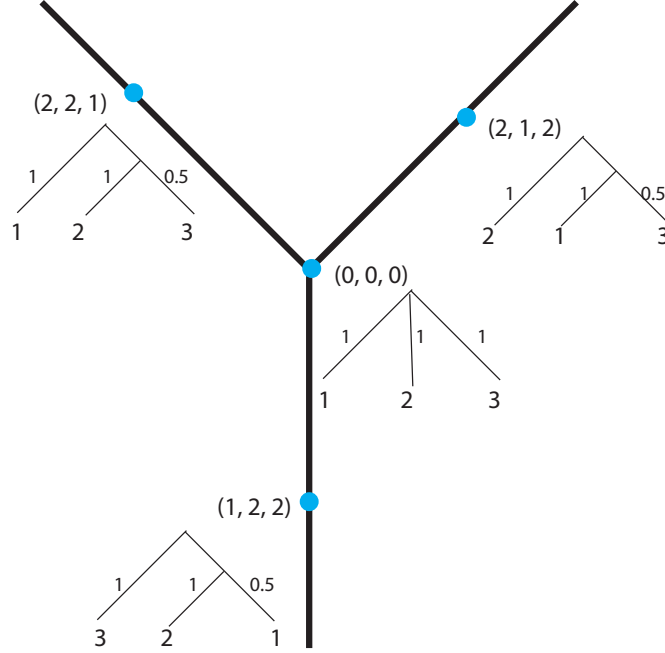


Figure 2: The space of ultrametrics for $m = 3$. Blue dots correspond to the equidistant trees shown in the figure.

Theorem 3.2. *Let $\mathcal{P} = tconv(D^{(1)}, \dots, D^{(s)}) \subseteq \mathbb{R}^e / \mathbb{R}\mathbf{1}$ be a tropical polytope spanned by ultrametrics. Then any two points x and y in the same cell of \mathcal{P} are also ultrametrics with the same tree topology.*

Proof. Because the space of ultrametrics \mathcal{U}_m is a tropical linear space, so is tropically convex, \mathcal{P} is contained in \mathcal{U}_m . Hence any points x and y in \mathcal{P} must also be ultrametrics.

Let S be the type of x and y . To check whether x and y have the same tree topology, we check the three point condition for each trio of leaves. Fix such a trio i, j , and k . Our first claim is that $x_{ij} = x_{ik} = x_{jk}$ if and only if $y_{ij} = y_{ik} = y_{jk}$. To see why, suppose the former is true. Because $x \in \mathcal{P}$, there exists some index $a \in S_{ij}$, so that

$$D_{ij}^{(a)} - x_{ij} = \max_{\ell_1 < \ell_2} D_{\ell_1, \ell_2}^{(a)} - x_{\ell_1, \ell_2}.$$

In particular, $D_{ij}^{(a)} - x_{ij} \geq D_{ik}^{(a)} - x_{ik}$ and $D_{ij}^{(a)} - x_{ij} \geq D_{jk}^{(a)} - x_{jk}$. By assumption it follows that $D_{ij}^{(a)} \geq D_{ik}^{(a)}$ and $D_{ij}^{(a)} \geq D_{jk}^{(a)}$. Because $D^{(a)}$ is an ultrametric, the maximum among $D_{ij}^{(a)}, D_{ik}^{(a)}, D_{jk}^{(a)}$ is attained twice, so one of these is actually an equality. Without loss of generality, let $D_{ij}^{(a)} = D_{ik}^{(a)}$. Then $D_{ij}^{(a)} - x_{ij} = D_{ik}^{(a)} - x_{ik}$ and $a \in S_{ik}$ as well.

Recall that S is also the type of y . This means

$$D_{ij}^{(a)} - y_{ij} = D_{ik}^{(a)} - y_{ik} = \max_{\ell_1 < \ell_2} D_{\ell_1, \ell_2}^{(a)} - y_{\ell_1, \ell_2}.$$

In particular, since $D_{ij}^{(a)} = D_{ik}^{(a)}$, we have $y_{ij} = y_{ik}$ as well. The same argument applied to S_{jk} shows that $y_{jk} = y_{ij}$ or $y_{jk} = y_{ik}$; it follows that $y_{ij} = y_{ik} = y_{jk}$ as desired.

Now suppose $\max(x_{ij}, x_{ik}, x_{jk})$ and $\max(y_{ij}, y_{ik}, y_{jk})$ are both attained exactly twice. We claim that the minimum for x and for y is attained for the same pair of leaves. Suppose without loss of generality that $x_{ij} = \min(x_{ij}, x_{ik}, x_{jk})$ and $y_{ik} = \min(y_{ij}, y_{ik}, y_{jk})$: because $x, y \in \mathcal{P}$, there exists some index $a \in S_{jk}$. This implies in particular that $D_{jk}^{(a)} - x_{jk} \geq D_{ij}^{(a)} - x_{ij}$ and $D_{jk}^{(a)} - y_{jk} \geq D_{ik}^{(a)} - y_{ik}$.

Rearranging these inequalities produces $D_{jk}^{(a)} - D_{ij}^{(a)} \geq x_{jk} - x_{ij}$ and $D_{jk}^{(a)} - D_{ik}^{(a)} \geq y_{jk} - y_{ik}$. Since $x_{ij} < x_{jk}$ and $y_{ik} < y_{jk}$ by assumption, it follows that $D_{jk}^{(a)}$ must be the unique maximum among $D_{ij}^{(a)}, D_{ik}^{(a)}, D_{jk}^{(a)}$, a contradiction because $D^{(a)}$ is ultrametric. \square

See Figures 8 and 9 for illustrations of this result.

It is natural to ask when a tropical PCA contains the origin: i.e., when the fully unresolved phylogenetic tree is contained in the PCA. This question turns out to have a simple answer.

Lemma 3.3. *Let $\mathcal{P} = \text{tconv}(D^{(1)}, \dots, D^{(s)}) \subseteq \mathbb{R}^e / \mathbb{R}\mathbf{1}$ be a tropical polytope spanned by ultrametrics. The origin $\mathbf{0}$ is contained in \mathcal{P} if and only if the path between each pair of leaves i, j passes through the root of some $D^{(i)}$.*

Proof. The $D^{(i)}$ can certainly be tropically scaled to have largest coordinate 0. If the claimed condition holds, then the sum of these scaled $D^{(i)}$ will be the origin as desired.

Suppose $\mathbf{0}$ is contained in \mathcal{P} , meaning we can write $\mathbf{0} = \bigoplus a_i \odot D^{(i)}$. Consider some pair of leaves i, j . This must appear as the coordinate of some $a_k \odot D^{(k)}$. Because $\mathbf{0} = \bigoplus a_i \odot D^{(i)}$, all other coordinates of $a_k \odot D^{(k)}$ must be non-positive, meaning that the i, j coordinate of $a_k \odot D^{(k)}$ is maximal as desired. \square

Definition 3.4. *Suppose we have a sample $\{D^{(1)}, \dots, D^{(n)}\}$. A Fermat-Weber point x^* of $\{D^{(1)}, \dots, D^{(n)}\}$ is a minimizer of the sum of tropical distances to the data points:*

$$x^* := \arg \min_x \sum_{i=1}^n d_{\text{tr}}(x, D^{(i)}).$$

We can naturally view Fermat-Weber points as zero-dimensional PCAs.

Lemma 3.5. *Suppose $n \geq 3$ and $\{D^{(1)}, \dots, D^{(n)}\} \subset \mathcal{U}_m$. Then there exists a Fermat-Weber point x^* of the dataset lying in the tropical polytope $\text{tconv}(D^{(1)}, \dots, D^{(n)})$. In particular, this point x^* is ultrametric.*

Proof. Take x^* a Fermat-Weber point not lying in $\text{tconv}(D^{(1)}, \dots, D^{(n)})$, and let $S = (S_1, \dots, S_e)$ be its vector of types as in Definition 2.6. Because x^* does not lie in the tropical polytope, some of the types S_j are empty. Consider such an S_j . By definition, we have that for each i , $D_j^{(i)} - x_j^*$ is not maximal among $\{D_1^{(i)} - x_1^*, \dots, D_e^{(i)} - x_e^*\}$. This also means that we can shift the j th coordinate without changing the distance of x^* to any datapoint $D^{(i)}$. We can therefore simply decrease x_e^* until there is some i such that $D_j^{(i)} - x_j^*$ is tied for being maximal among the coordinates of $D^{(i)} - x^*$. The tropical type S_j of our new x^* will be nonempty. By doing so for all coordinates, we obtain a new Fermat-Weber point which lies in the tropical polytope spanned by ultrametrics and so is itself ultrametric. \square

The previous lemma states that there always exists a biologically interpretable zero-dimensional tropical PCA for a dataset of ultrametrics. This result points toward the following conjecture, which is analogous to the classical fact that the s -dimensional PCA is contained in the t -dimensional PCA if $s \leq t$.

Conjecture 3.6. *There exists a tropical Fermat-Weber point $x^* \in \mathcal{U}_m$ of a sample $D^{(1)}, \dots, D^{(n)}$ of ultrametric trees which is contained in the s th order tropical PCA of the dataset for $s \geq 1$.*

4 Methods

In this section we discuss how to estimate the optimal solution to a tropical PCA via a Markov Chain Monte Carlo (MCMC). This can be applied to estimate the $(s - 1)$ -th order principal components for $s \geq 1$.

In the remainder of this paper we often focus on $s = 3$ for simplicity, even though our techniques apply for any $s \geq 3$. Finding the 3rd order tropical PCA can be written as the following optimization problem:

Problem 4.1. *We seek a solution for the following optimization problem:*

$$\min_{D^{(1)}, D^{(2)}, D^{(3)} \in \mathcal{U}_m} \sum_{i=1}^n d_{\text{tr}}(u_i, u'_i)$$

where

$$u'_i = \lambda_1^i \odot D^{(1)} \oplus \lambda_2^i \odot D^{(2)} \oplus \lambda_3^i \odot D^{(3)}, \quad \text{where } \lambda_k^i = \min(u_i - D^{(k)}), \quad (3)$$

and

$$d_{\text{tr}}(u_i, u'_i) = \max\{|u_i(k) - u'_i(k) - u_i(l) + u'_i(l)| : 1 \leq k < l \leq e\} \quad (4)$$

with

$$u_i = (u_i(1), \dots, u_i(e)) \text{ and } u'_i = (u'_i(1), \dots, u'_i(e)). \quad (5)$$

Let $\Pi_\Delta(S) := \sum_{i=1}^{|S|} d_{\text{tr}}(u_i, u'_i)$, where $S = \{u_1, \dots, u_n\}$ with $u_i \in \mathbb{R}^e / \mathbb{R}\mathbf{1}$ are ultrametrics and u'_i is the tropical projection of u_i onto a tropical triangle Δ .

The following algorithm computes a proposal state, i.e., a set of proposed trees.

Algorithm 4.2 (Finding the proposal set of trees).

- *Input:* Set of equidistant trees $\{T_1, T_2, T_3\}$, $k \in [m]$.
- *Output:* Next set of equidistant trees $\{T'_1, T'_2, T'_3\}$.

for $i = 1, \dots, 3$ **do**

Set $T'_i = T_i$.

Pick random numbers $(i_1, \dots, i_k) \subset [m]$ without replacement.

Permute the tree leaf labels $(i_1, \dots, i_k) \subset [m]$ of T'_i with a random permutation σ in the symmetric group on $\{i_1, \dots, i_k\}$.

Pick a random internal branch b_1 in T'_i with branch length l_i .

Update $l_i := l_i + \epsilon \cdot c$ where $\epsilon \sim \text{Unif}\{\pm 1\}$, and $c \sim \text{Unif}[0, l_i/m]$.

Pick another branch b_2 with branch length l on the path from the root to a leaf where the branch b_1 is also on the path.

If $l - \epsilon \cdot c < 0$ then set $l := 0$ and $l_i := l_i + l - \epsilon \cdot c$. If not then set $l := l - \epsilon \cdot c$.

end for

Return $\{T'_1, T'_2, T'_3\}$.

Next we use the Metropolis algorithm to decide whether the proposal state should be accepted or rejected. Let $\Delta_{(w_1, w_2, w_3)}$ be the tropical triangle spanned by w_1, w_2, w_3 .

Algorithm 4.3 (Metropolis algorithm).

- *Input:* Current set of equidistant trees $\{T_1, T_2, T_3\}$ and the proposal state, $\{T'_1, T'_2, T'_3\}$. The sample of ultrametrics $S = \{u_1, \dots, u_n\}$.
- *Output:* Decision whether we should accept the proposal or not.

Compute ultrametrics w_1, w_2, w_3 , from T_1, T_2, T_3 , respectively.

Compute ultrametrics v_1, v_2, v_3 , from T'_1, T'_2, T'_3 , respectively.

Compute $\Pi_{\Delta_{w_1, w_2, w_3}}(S)$ and $\Pi_{\Delta_{v_1, v_2, v_3}}(S)$.

Set $p = \min\{1, \Pi_{\Delta_{w_1, w_2, w_3}}(S)/\Pi_{\Delta_{v_1, v_2, v_3}}(S)\}$.

Accept a proposal $\{T'_1, T'_2, T'_3\}$ with probability p .

Piecing together Algorithms 4.2 and 4.3, we have the following MCMC algorithm.

Algorithm 4.4 (MCMC algorithm to estimate the second order principal components).

- *Input:* Sample of equidistant trees $\{T_1, \dots, T_n\}$. Constant positive integer $C > 0$.
- *Output:* Second order principal components $\{T_1^*, T_2^*, T_3^*\}$.

Set $S := \{u_1, \dots, u_n\}$ where d_i is the ultrametrics computed from a tree T_i , for $i = 1, \dots, n$.

Pick random trees $\{T_0^1, T_0^2, T_0^3\} \subset \{T_1, \dots, T_n\}$ and compute ultrametrics w_1^*, w_2^*, w_3^* respectively.

Set $i = 1$, $k = m$, where m is the number of leaves.

repeat

if $i \bmod C$ equals zero and $k > 0$ **then**

 set $k = k - 1$.

end if

 Compute the proposal $\{T_1^1, T_1^2, T_1^3\}$ via Algorithm 4.2 with $\{T_0^1, T_0^2, T_0^3\}$ and k .

 Compute ultrametrics w_1, w_2, w_3 , from T_1^1, T_1^2, T_1^3 , respectively.

if Algorithm 4.3 returns ‘‘accept’’ **then**

 Set $T_0^1 = T_1^1$, $T_0^2 = T_1^2$, and $T_0^3 = T_1^3$.

end if

if $\Pi_{\Delta_{w_1, w_2, w_3}}(S) < \Pi_{\Delta_{w_1^*, w_2^*, w_3^*}}(S)$ **then**

 set $w_1^* := w_1$, $w_2^* := w_2$, $w_3^* := w_3$.

end if

 Set $i = i + 1$.

until Converges

Return the ultrametrics w_1^, w_2^*, w_3^* .*

4.1 Fraction of variance of unexplained and variance of explained

To analyze the fit of a tropical PCA to the observed data, we used a fraction of variance of unexplained $\Pi_\Delta(S)$ and variance of explained in terms of our tropical geometric set up. In tropical geometry, it is natural to use a Fermat-Weber point as a centroid of the given datasets [Lin et al. (2017)], and correspondingly we will use a sum of tropical distances instead of the squared distances. Let S_{reg} be the “variance of explained”, defined as

$$S_{reg} = \sum_{i=1}^n d_{tr}(\hat{u}_i, \bar{u})$$

where \hat{u}_i is the tropical projection of an ultrametric u_i for a tree T_i in the input sample onto a tropical polytope and \bar{u} is a Fermat Weber point of $\{\hat{u}_1, \dots, \hat{u}_n\}$ as defined in Section 3.

We define the fraction of variance of unexplained as

$$\frac{\Pi_\Delta(S)}{\Pi_\Delta(S) + S_{reg}}.$$

Here the coefficient of determination (or the proportion of the variance of explained), or R^2 , is defined as

$$R^2 = 1 - \frac{\Pi_\Delta(S)}{\Pi_\Delta(S) + S_{reg}} = \frac{S_{reg}}{\Pi_\Delta(S) + S_{reg}}. \quad (6)$$

We use the proportion of determination R^2 as the statistic to measure how well the model fits to the given data.

5 Verifications

5.1 Mixture of coalescent models

For the first simulation study, we generated gene trees with a species tree under a coalescent model via the software **Mesquite** [Maddison and Maddison (2018)]. We fixed the effective population size $N_e = 100,000$ and varied

$$r = \frac{SD}{N_e}$$

where SD is the species depth.

Algorithm 5.1 (Sample gene trees from a coalescent model).

- *Input:* The number of gene trees n , labels of leaves $\{1, \dots, m\}$, effective population size N_e and species depth SD .
- *Output:* A sample of n gene trees with a fixed species tree T_s under a coalescent model.

Generate a species tree T_s with the label $\{1, \dots, m\}$ and N_e under Yule model.

*Generate n many gene trees with T_s and N_e under the coalescent model via **Mesquite**.*

Return the gene trees generated and T_s .

This experiment is to generate two distributions of gene trees under the coalescent model with different species trees using Algorithm 5.1. Then we use Algorithm 5.2 to compute a tropical PCA on the mixture of these two distributions generated. In these simulated experiments, we have varied the ratio $r = 0.25, 0.5, 1, 2, 5, 10$. We also fix the number of leaves $m = 10$.

Algorithm 5.2 (PCA with two distributions of gene trees with difference species trees).

- *Input:* $S_1 := \{T_1, \dots, T_n\}$, a sample of gene trees generated with a species tree T_{S_1} and $S_2 := \{T'_1, \dots, T'_n\}$, a sample of gene trees generated with a species tree T_{S_2} where $T_{S_1} \neq T_{S_2}$.
- *Output:* PCA (second PCs) with a sample $\{T_1, \dots, T_n, T'_1, \dots, T'_n\}$.

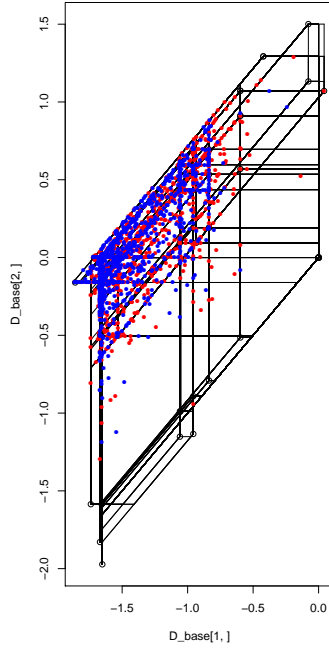
Apply a tropical PCA and compute the second order principal components with $\{T_1, \dots, T_n, T'_1, \dots, T'_n\}$.

Color red for the projected points of $\{T_1, \dots, T_n\}$ onto the tropical PCA and color blue for for the projected points of $\{T'_1, \dots, T'_n\}$ onto the tropical PCA.

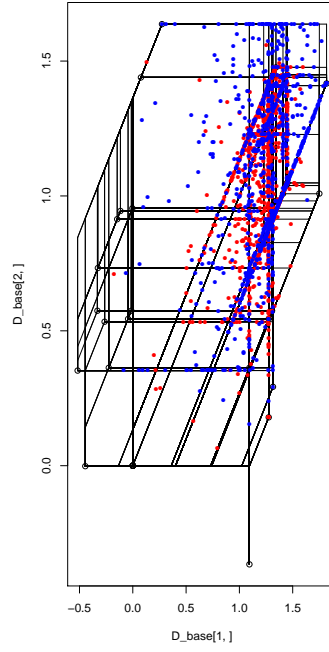
In order to compare our results, we also applied the same simulated data sets to **geophytter** which approximate the BHV PCA on the BHV tree space [Nye et al. (2017)]. To compare the accuracy rates we use R^2 , the variance of explained. Note that the R^2 statistic for the BHV PCA is defined in an analogous way to our R^2 , simply replacing the tropical distance with the BHV distance.

5.2 Sensitivity analysis

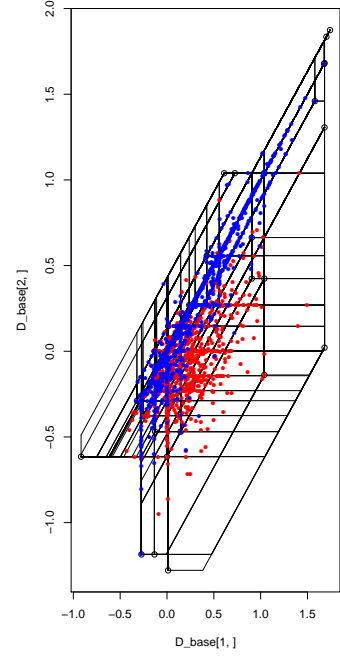
For the second simulation study, we worked on sensitivity analysis of our MCMC method for estimating tropical PCA from the given data. Also with simulated data we study a convergence rate of our MCMC approach.



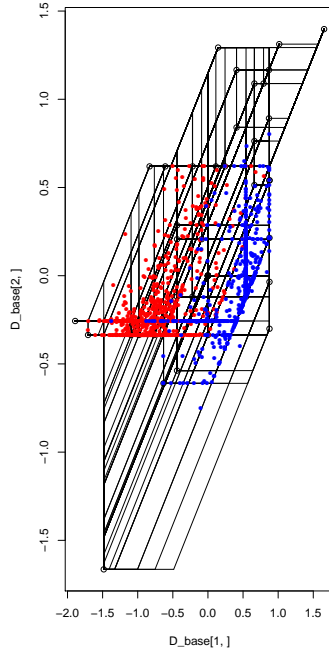
(a) $r = 0.25$.



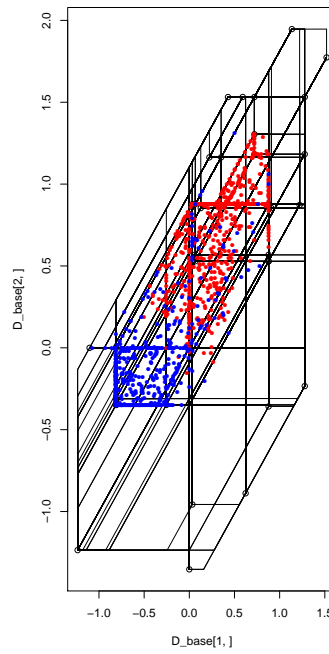
(b) $r = 0.5$.



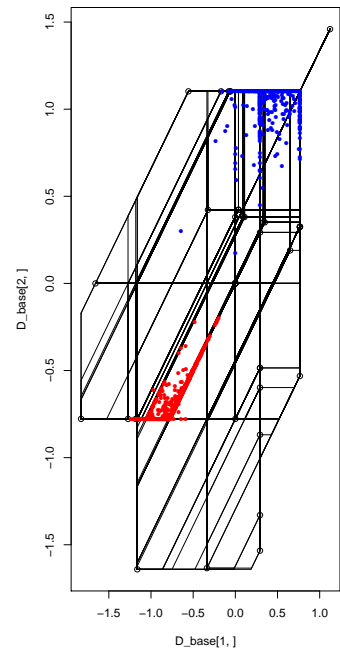
(c) $r = 1$.



(d) $r = 2$.



(e) $r = 5$.



(f) $r = 10$.

Figure 3: We applied tropical PCAs on the mixture of two coalescent distributions using Algorithm 5.1. We colored blue for projected trees whose gene trees are generated from one coalescent distribution and red for the other distribution. We varied the ratio r .

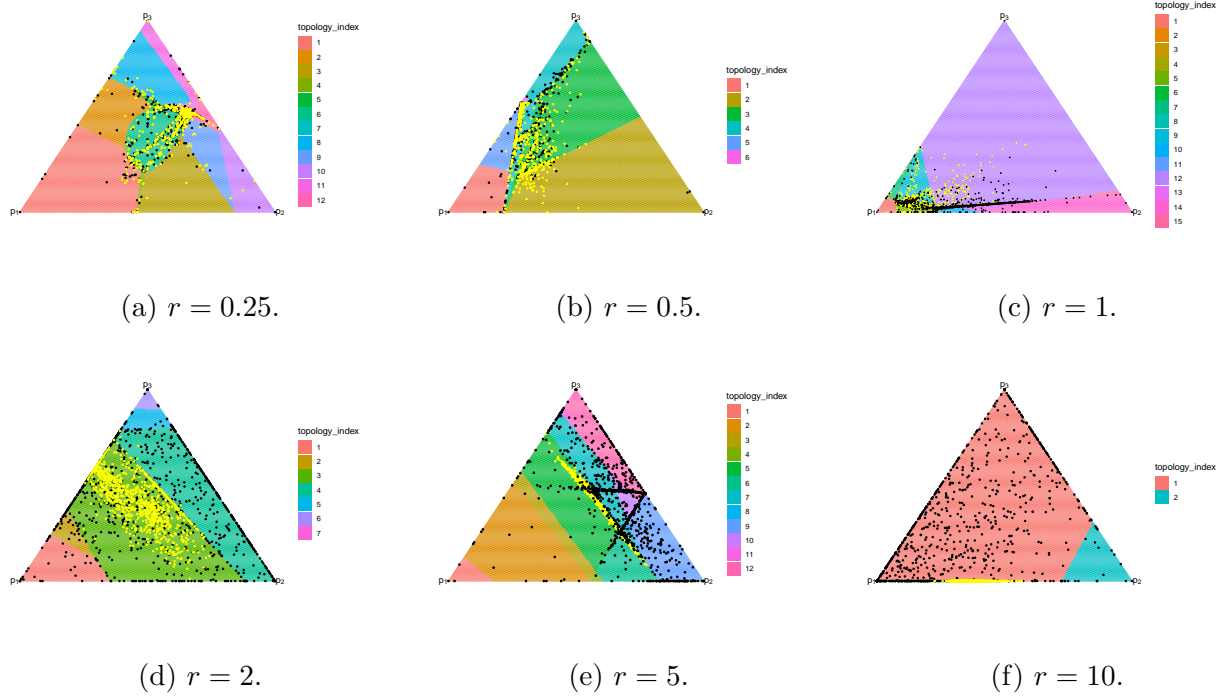


Figure 4: We applied BHV PCAs on the mixture of two coalescent distributions. We colored black for projected trees whose gene trees are generated from one coalescent distribution and yellow for the other distribution. We varied the ratio r .

r	Tropical PCA	BHV PCA
0.25	0.316	0.009
0.5	0.297	0.009
1	0.186	0.042
2	0.319	0.034
5	0.278	0.009
10	0.396	0.009

Table 1: R^2 for the tropical PCAs and the BHV PCAs for the mixtures of two coalescent distributions.

For a sensitivity analysis, we run our MCMC approach 10 times on the same set of data (fixed the number of leaves, the number of trees, and the number of iterations for each MCMC) and see how the vertices of the tropical PCA and corresponding R^2 change. For a convergence rate, we plot R^2 varying the number of iterations on each MCMC run.

We conducted these simulations on a set of random tree topologies and a set of datapoints of fixed tree topology. The parameters for this simulation study are listed in Table 2. For each case, we ran ten Markov chains.

Parameter	
Tree topology	random or fixed tree topology
Number of leaves	4, ..., 9
Number of trees	5, 25, 50, 100, 1000
Number of iterations	10, 100, 1000, 10000

Table 2: Parameters set up for the second simulation study.

5.2.1 Fixed tree topology

We fixed the equidistant tree topology shown in Figure 5. The biggest external edge from the leaf 1 to its root has its branch length 1.

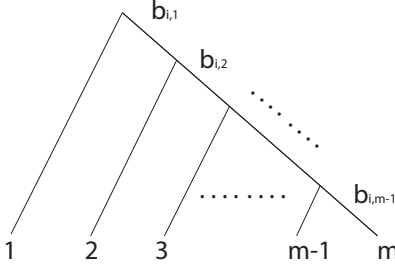


Figure 5: The fixed equidistant tree topology for the second simulation study.

We generate a set of random equidistant trees with this fixed tree topology shown in Figure 5 by Algorithm 5.3.

Algorithm 5.3 (Generating random equidistant trees with the fixed tree topology shown in 5).

- *Input: The number of leaves m and sample size n .*
- *Output: n many random trees with the fixed tree topology with m leaves.*

for $i = 1, \dots, n$ **do**

Generate an equidistant tree T_i with its topology shown in 5.

Let $b_{i,1}, \dots, b_{i,m-1}$ be interior edges in T_i shown in Figure 5. Let $l(b_{i,j})$ is the branch length of the edge $b_{i,j}$.

for $j = 1, \dots, m - 1$ **do**

Pick a random number u uniformly $[0, 1 - (\sum_{k=1}^{j-1} l(b_{i,k}))]$.

Assign $l(b_{i,j}) = u$.

end for

for $j = 1, \dots, m - 1$ **do**

Assign the branch length for the external edge adjacent to a leaf j equal to $\sum_{k=j}^{m-1} l(b_{i,k})$.

end for

end for

Return $\{T_1, \dots, T_n\}$.

The simulation results can be found in Figure 6 below. Note that even though we fix the tree topology the branch lengths are random. Therefore, in general R^2 should be low. In addition,

from the figure note that the more iterations for a Markov chain correlates with a higher R^2 . Also from the figure the variation of R^2 is smaller when the number of iterations increases. This implies that a MCMC is converging to a local or global optima. Since the variance is very small for some cases, a Markov chain seems to converge to a global optima for these cases. From this experiments, a Markov chain is quickly converging to a local or global optima very quickly. Also in general when the number of leaves is smaller we have higher R^2 because the dimension of the tree space is smaller; similarly when the number of trees is smaller we also have a higher R^2 .

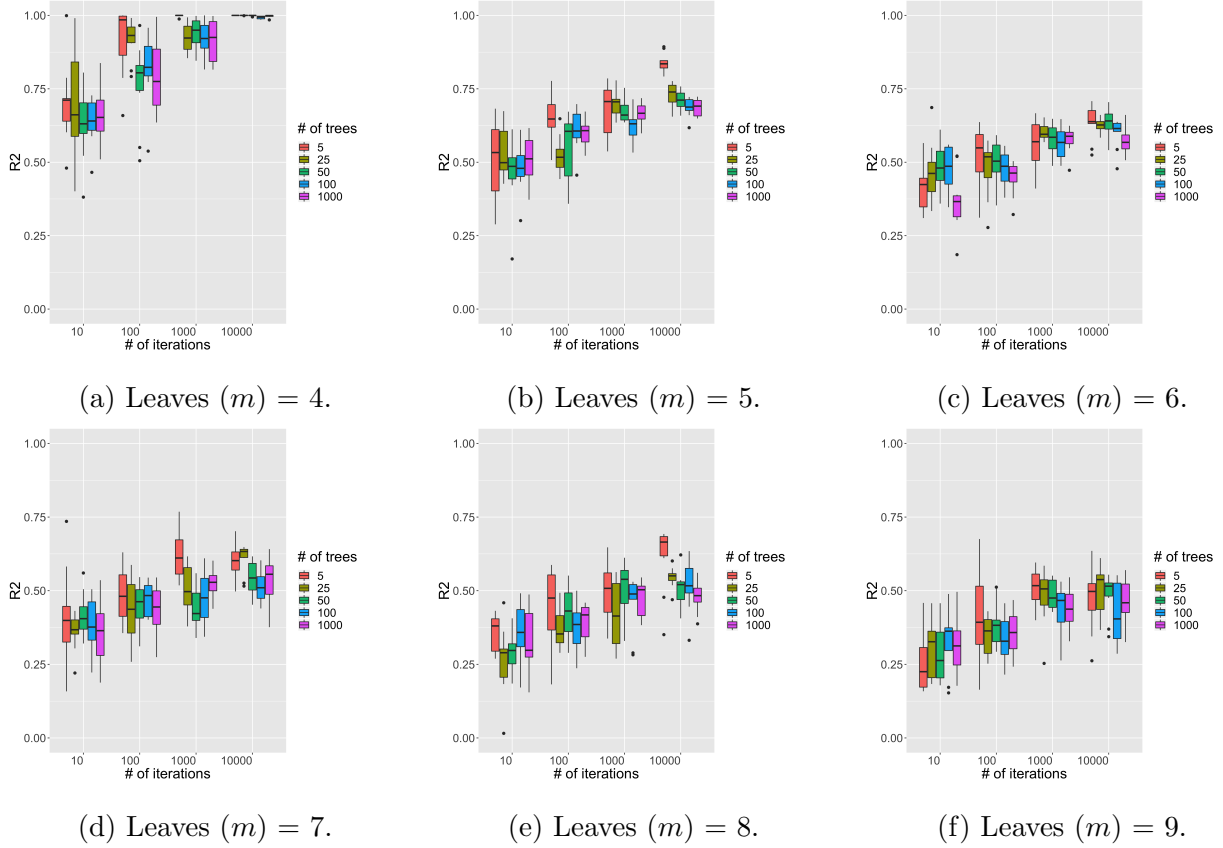


Figure 6: We applied the MCMC approach to compute a tropical PCA on the datasets generated by Algorithm 5.3 with the parameters listed in Table 2. We ran 10 Markov chains and we computed a box plot for each case. The y-axis represents R^2 and the x-axis represents the number of iterations for a MCMC.

5.2.2 Random tree topology

For this simulation we used `rcoal()` function from `ape` package in R with fixed height equal to one. The simulation results can be found in Figure 7 below. Note that since trees are all random, in general R^2 should be much lower compared to R^2 computed from the samples of ultrametrics with the same tree topologies. The overall trends of R^2 are similar to the ones with the fixed tree topology.

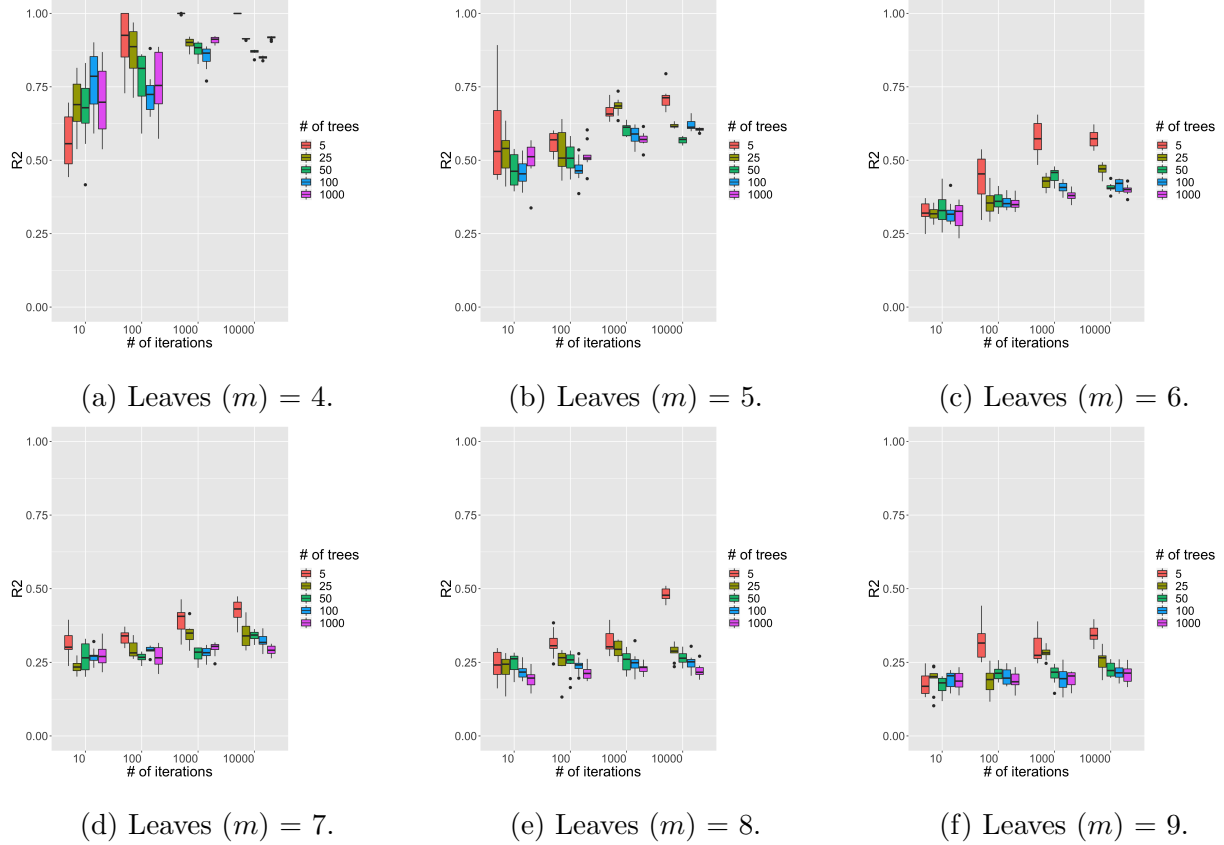
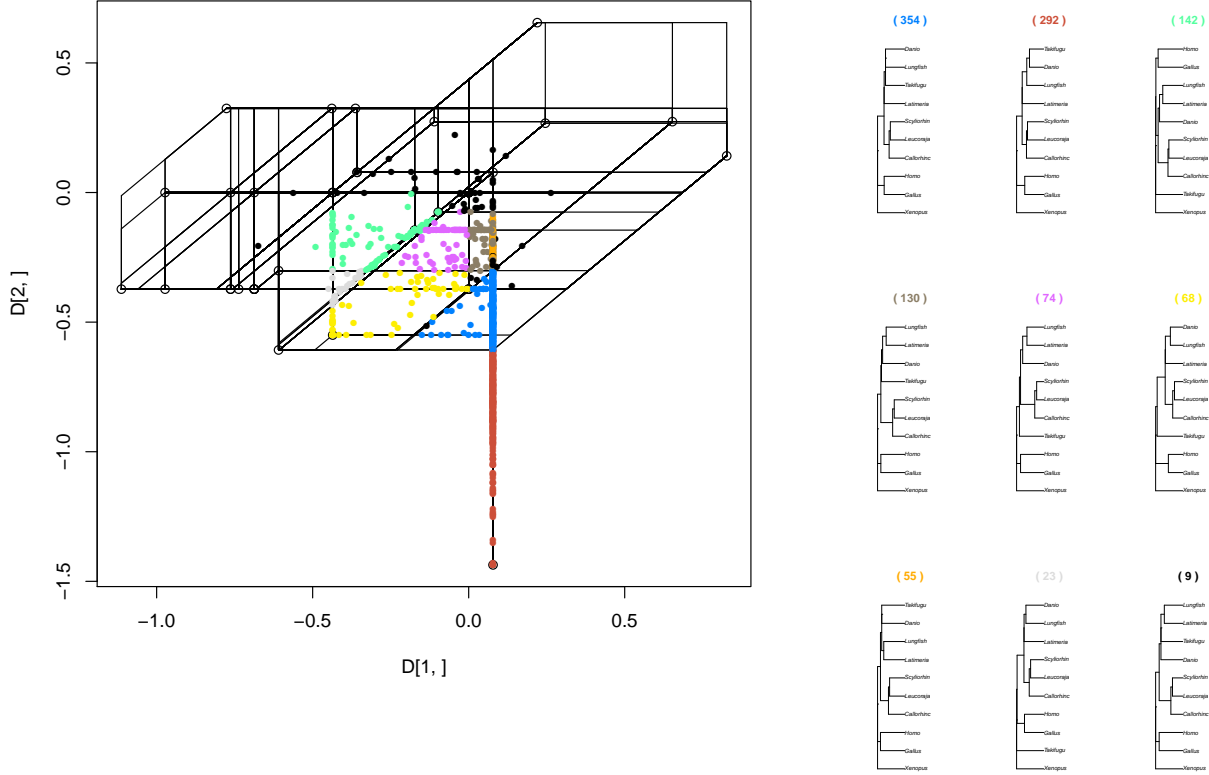


Figure 7: We applied the MCMC approach to compute a tropical PCA on the datasets of random trees with the parameters listed in Table 2. The y-axis represents R^2 and the x-axis represents the number of iterations for a MCMC.

6 Empirical data

We applied our method to three empirical data sets: Apicomplexa gene trees [Kuo et al. (2008)], the African coelacanth genome [Liang, et al. (2013)], and flu virus data [Zairis et al. (2016)].



(a) Second order tropical PCA for African coelacanth genome data. Black colored dots are trees with the tree topologies with frequencies in the lower 5 percentile.

(b) Tree topologies projected on the tropical PCA.

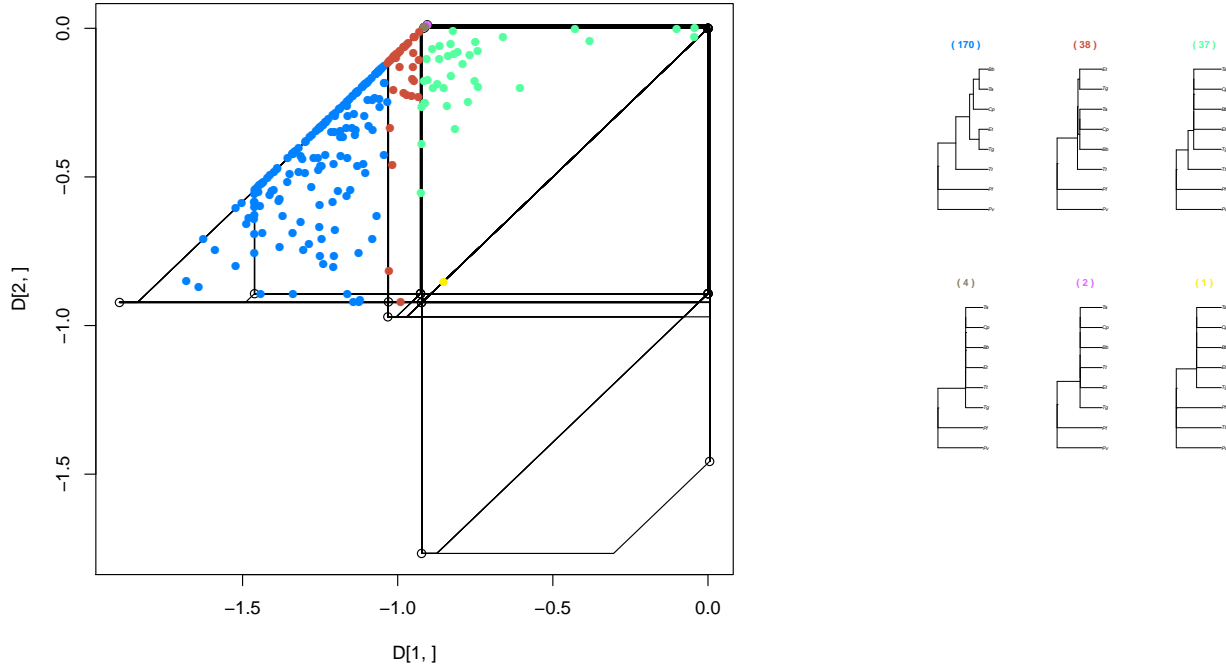
Figure 8: Estimated tropical PCA of African coelacanth genome data via our MCMC method.

6.1 African coelacanth genome data

We applied our MCMC technique to estimate the tropical PCA to the dataset consisting of 1,290 genes on 690,838 amino acid residues obtained from genome and transcriptome data [Liang, et al. (2013)]. The result is shown in Figure 8. In Figure 8 each tree topology of a projection onto the second order tropical PCA has a color and black color represents tree topologies in the lower five percentile.

6.2 Apicomplexa

The second empirical dataset we have applied is from 268 orthologous sequences with eight species of protozoa presented in [Kuo et al. (2008)]. This data set has gene trees reconstructed from the



(a) Second order tropical PCA for Apicomplexa gene data. Black colored dots are trees with the tree topologies with frequencies in the lower 5 percentile.

(b) Tree topologies projected on the tropical PCA.

Figure 9: Estimated tropical PCA of gene trees on Apicomplexa data set via our MCMC method.

following sequences: *Babesia bovis* (Bb), *Cryptosporidium parvum* (Cp), *Eimeria tenella* (Et) [15], *Plasmodium falciparum* (Pf) [11], *Plasmodium vivax* (Pv), *Theileria annulata* (Ta), and *Toxoplasma gondii* (Tg). An outgroup is a free-living ciliate, *Tetrahymena thermophila* (Tt).

The result is shown in Figure 9. In Figure 9 each tree topology of a projection onto the second order tropical PCA has a color and black color represents tree topologies with their frequencies in the lower five percentile.

6.3 Flu virus data set

We have applied our MCMC approach to estimate a tropical second order PCA to a genomic data for 1089 full length sequences of hemagglutinin (HA) for influenza A H3N2 from 1993 to 2017 in the state of New York were obtained from the GI-SAID EpiFluTM database (www.gisaid.org).

org). The data were aligned with MUSCLE [Edgar (2004)] with the default settings. Then a *tree dimensionality reduction* [Zairis et al. (2016)] was applied via windows of 5 consecutive seasons to create 21 datasets. The year of each dataset corresponds to the first season. We have applied the neighbor-joining method [Saitou and Nei (1987)] with p-distance to reconstruct each tree in the datasets. Outliers were then removed from each season using KDETREES [Weyenberg et al. (2014)]. Each sample size is about 20,000 (see Table 3 for details).

In this experiment we applied our MCMC approach to these datasets and we compared our results with a PCA via BHV metric developed by Nye et al [Nye et al. (2017)]. The results of our computational experiments can be found in Table 4.

7 Conclusion

This paper provides theoretical background for the interpretation of tropical PCAs on the space of ultrametrics and introduces a our novel stochastic method using a Metropolis-Hastings algorithm to search phylogenetic tree space.

We successfully implement our innovative MCMC tropical PCA approach on three empirical datasets, Apicomplexa, African coelacanth genomes, and HA sequences of influenza virus. Our results for all of them are notable. Each plot shows a tight cluster, implying that the use of gene trees to infer species topology is valid. The strong R^2 values suggest our second order tropical PCA approach is effectively reducing gene tree dimensions. The inferential topologies for the species tree are nearly identical, strengthening the proof of our hypothesis. For African coelacanth genomes data, from our tropical PCA Lung fish is closest to the tetrapods in the tree topology of the projected trees onto the tropical PCA with the highest frequency. This is consistent with the result found in [Liang, et al. (2013)]. In addition for Apicomplexa data, out tropical PCA shows that the tree topology of the projected trees onto the tropical PCA is the same as the species tree reconstructed by [Kuo et al. (2008)]. These results show that our method to estimate the tropical PCA works well with these empirical data.

Future research could consider model and visualization improvements. Streamlining the tropical MCMC implementation in R, specifically the coding, will improve efficiency and usability. There is room for improvements in the heating and cooling of the MCMC function, which will increase effectiveness of the tropical PCA algorithm. Further exploration is necessary to understand

Year	Tree with 4 leaves		Tree with 5 leaves	
	Before	After	Before	After
1993	20000	20000	20890	20890
1994	20000	20000	20000	20000
1995	20000	20000	20000	20000
1996	20000	20000	20000	20000
1997	20000	20000	20000	20000
1998	20000	20000	20000	20000
1999	20000	20000	20000	20000
2000	20000	20000	20000	20000
2001	20000	20000	20000	19997
2002	20000	19995	20000	19910
2003	20000	20000	20000	20000
2004	20000	20000	20000	20000
2005	20000	20000	20000	20000
2006	20000	20000	20000	20000
2007	20000	20000	20000	19118
2008	6030	5887	20000	20000
2009	4590	4590	20000	20000
2010	20000	20000	20000	20000
2011	20000	20000	20000	19366
2012	21411	21411	20000	19876
2013	20000	19957	20000	19996
2014	20000	20000	N/A	N/A

Table 3: The sample sizes for flu virus dataset

the best starting set of trees for the tropical triangle.

Clearer and more meaningful visualization improves interpretability of tropical PCA results. For example, the tropical line segments in our plots correspond to tree topologies; however, iden-

Year	Tree with 4 leaves		Tree with 5 leaves	
	Tropical PCA	BHV	Tropical PCA	BHV
1993	0.9981 (0.9559)	0.7099	0.8962 (0.7269)	0.3019
1994	0.9997 (0.9426)	0.4611	0.9559 (0.8505)	0.4347
1995	0.9999 (0.8665)	0.19	0.9787 (0.9577)	0.3151
1996	0.9997 (0.9821)	0.215	0.9851 (0.7482)	0.5025
1997	0.9930 (0.9532)	0.0069	0.9430 (0.8437)	0.0505
1998	>0.9999 (0.9395)	0.0452	0.9264 (0.879)	0.6408
1999	>0.9999 (0.9069)	0.0038	0.9798 (0.8564)	0.9524
2000	0.9892 (0.9132)	0.9555	0.9302 (0.794)	0.0014
2001	>0.9999 (0.9088)	0.9402	0.9526 (0.8302)	0.9488
2002	0.9995 (0.9863)	0.0107	0.9956 (0.9525)	0.8962
2003	0.9995 (0.9848)	0.0972	0.9685 (0.8622)	0.4927
2004	0.9982 (0.9505)	0.4272	0.9502 (0.7931)	0.3651
2005	0.9998 (0.9949)	0.4628	0.9770 (0.8304)	0.3634
2006	0.9972 (0.9643)	0.0951	0.8350 (0.73)	0.2383
2007	0.9926 (0.9381)	0.5562	0.8912 (0.6995)	0.2727
2008	0.9920 (0.8813)	0.4887	0.7753 (0.4637)	0.0460
2009	0.9860 (0.8926)	0.0763	0.9034 (0.6289)	0.1563
2010	0.9995 (0.8886)	0.0329	0.8603 (0.6665)	0.1935
2011	0.9999 (0.9016)	0.3592	0.6888 (0.5920)	0.2771
2012	0.9930	0.2756	0.7177(0.5568)	0.1998
2013	0.9499 (0.7935)	0.3612	0.7433 (0.5624)	0.1279
2014	0.9727	0.1383	N/A	N/A

Table 4: R^2 for flu virus dataset. R^2 for the tropical metric is measured via the formula in the equation (6) and for BHV is measured by the formula defined in [Nye et al. (2017)]. R^2 inside of parentheses are computed via a heuristic method in [Monod et al. (2019)].

tifying those tree topologies takes significant effort. Additionally, producing three-dimensional plots would greatly improve quality. A better understanding of tropical tree space and the mapping of the space to tree topologies may enable further application of tropical PCA techniques to phylogenetics.

References

- [Akian et al. (2011)] Akian, M., S. Gaubert, N. Violel and I. Singer. (2011). Linear Algebra Appl. *Best approximation in max-plus semimodules* **435** 3261–3296.
- [Billera, et al. (2001)] Billera, L., S. Holmes and K. Vogtman (2001). Advances in Applied Mathematics **27** 733–767. *Geometry of the space of phylogenetic trees.*
- [Cohen et al. (2004)] Cohen, G., S. Gaubert and J.P. Quadrat (2004). Linear Algebra Appl. **379** 395–422. *Duality and separation theorems in idempotent semimodules,*
- [Develin and Sturmfels (2004)] M. Develin and B. Sturmfels (2004). Documenta Math. **9** 1–27. *Tropical convexity.*
- [Edgar (2004)] Edgar, R. C. (2004). Nucleic Acids Res, **32** 1792–1797. *MUSCLE: multiple sequence alignment with high accuracy and high throughput,*
- [Joswig (2017)] Joswig, M. (2017). *Essentials of Tropical Combinatorics*, In preparation, <http://page.math.tu-berlin.de/~joswig/etc/index.html>
- [Kuo et al. (2008)] Kuo, C., J.P. Wares, and J.C. Kissinger (2008). Molec. Biol. Evol. **25**, 2689–98. *The Apicomplexan whole-genome phylogeny: An analysis of incongruence among gene trees.*
- [Liang, et al. (2013)] Liang, D., X.X. Shen, and P. Zhang (2013). Molec. Biol. Evol. **30**, 1803–7. *One thousand two hundred ninety nuclear genes from a genome-wide survey support lungfishes as the sister group of tetrapods.*
- [Lin et al. (2017)] Lin, B., B. Sturmfels, X. Tang, and R. Yoshida (2017). SIAM Discrete Math, **3**, 2015–2038. *Convexity in Tree Spaces,*

- [Maclagan and Sturmfels (2015)] Maclagan, D. and B. Sturmfels (2015). *Introduction to Tropical Geometry*, Graduate Studies in Mathematics, 161, American Mathematical Society, Providence, RI.
- [Maddison and Maddison (2018)] Maddison, W. P. and D. R. Maddison (2018). *Mesquite: a modular system for evolutionary analysis*. Version 3.51 <http://www.mesquiteproject.org>
- [Monod et al. (2019)] Monod, A., B. Lin, Q. Kang, and R. Yoshida (2019). *Tropical Foundations for Probability & Statistics on Phylogenetic Tree Space*, Available at <https://arxiv.org/abs/1805.12400>.
- [Nye, (2011)] Nye, T. (2011). *Annals of Statistics* **39** 2716–2739. *Principal components analysis in the space of phylogenetic trees*.
- [Nye et al. (2017)] Nye, T., X. Tang, G. Weyenberg and R. Yoshida (2017). *Biometrika* **104**, 901–922. *Principal Component Analysis and the Locus of the Fréchet Mean in the Space of Phylogenetic Trees*.
- [Paradis et al. (2004)] Paradis, E., J. Claude and K. Strimmer (2004). *Bioinformatics* **20**, 289–290. *APE: analyses of phylogenetics and evolution in R language*,
- [Saitou and Nei (1987)] Saitou, N. and M. Nei (1987). *The neighbor-joining method: a new method for reconstructing phylogenetic trees*. *Mol Biol Evol.* **4**, 406–25.
- [Weyenberg et al. (2014)] Weyenberg, G., P. Huggins, C. Schardl, D. Howe and R. Yoshida (2014). *Bioinformatics*, **30**, 2280–2287. *kdtrees: Nonparametric Estimation of Phylogenetic Tree Distributions*.
- [Yoshida et al. (2019)] Yoshida, R., L. Zhang and X. Zhang (2019). *Bulletin of Mathematical Biology.* **81**, 568–597. *Tropical Principal Component Analysis and its Application to Phylogenetics*.
- [Zairis et al. (2016)] S. Zairis, H. Khiabani, A.J. Blumberg, and R. Rabadán (2016). *Genomic Data Analysis in Tree Spaces*, available at arXiv:1607.07503.